



# Investigation of electronic coupling in semiconductor double quantum wells using coherent optical two-dimensional Fourier transform spectroscopy

Xiaoqin Li<sup>a,b</sup>, Tianhao Zhang<sup>a,c</sup>, Shaul Mukamel<sup>d</sup>, Richard P. Mirin<sup>e</sup>, Steven T. Cundiff<sup>a,\*</sup>

<sup>a</sup> JILA, University of Colorado and National Institute of Standards and Technology, Boulder, CO 80309-0440, USA

<sup>b</sup> Physics Department, University of Texas-Austin, Austin, TX, 78712, USA

<sup>c</sup> Department of Physics, University of Colorado, Boulder, CO 80309-0320, USA

<sup>d</sup> Chemistry Department, University of California, Irvine, CA, 92697-2025, USA

<sup>e</sup> National Institute of Standards and Technology, Boulder, CO 80305, USA

## ARTICLE INFO

### Article history:

Received 16 September 2008

Received in revised form

9 December 2008

Accepted 10 December 2008 by R. Merlin

Available online 24 December 2008

### PACS:

78.47.+p

### Keywords:

A. Semiconductors

A. Quantum wells

D. Optical properties

E. Nonlinear optics

## ABSTRACT

We investigate electronic coupling in asymmetric semiconductor double quantum wells using a new spectroscopy method, optical two-dimensional Fourier transform (2D-FT) spectroscopy. Measurements on two samples with different barrier thicknesses show drastically different 2D-FT spectra. We compare these measurements to conventional one-dimensional four-wave-mixing measurements, highlighting the unique advantages of the 2D-FT spectroscopy. An oscillatory behavior in the intensity of the cross peaks as a function of the mixing time is observed. This oscillation is attributed to interference between different quantum mechanical pathways, and its features are determined by the non-radiative Raman coherence between dipole-forbidden states.

© 2008 Elsevier Ltd. All rights reserved.

## 1. Introduction

Double-well potentials are encountered in many areas of physics, chemistry and biology. Examples include diffusion of defects in solids, structure relaxation in glasses, inversion of ammonia molecules, and proton tunneling between DNA base pairs. Epitaxially grown semiconductor double quantum wells (DQWs) provide a unique model system where electronic coupling strength and tunneling rate between the two wells can be easily and systematically varied by changing the barrier thickness. In DQWs, many intriguing phenomena, which are absent in single-well structures, arise from the competition between tunneling and recombination of electrons and holes [1–4]. Such dynamics become particularly interesting in the presence of quantum dissipation and decoherence. In addition, DQW structures are widely used in various opto-electronic devices. Electronic coupling between inter-well transitions is known to affect the electro-optical response in these structures [5]. Therefore, an improved understanding of electronic coupling in DQWs would allow

rational design of new and improved quantum-well-based opto-electronic devices.

In this paper, we use optical two-dimensional Fourier transform (2D-FT) spectroscopy to improve the understanding of electronic coupling by detecting it and qualitatively measuring the exciton coupling strength in DQWs. In addition, 2D-FT spectroscopy is capable of separating coherent coupling from incoherent relaxation processes. This capability is particularly useful in light of rising interest in semiconductor quantum devices operating solely in the coherent regime [6,7]. Prior to the development of 2D-FT spectroscopy, semiconductors were studied extensively using other forms of coherent spectroscopy [8]. We provide a comparison between 2D-FT and conventional spectroscopy methods in this paper.

Following concepts developed in nuclear magnetic resonance (NMR) spectroscopy [9], optical 2D-FT spectroscopy has been implemented to study vibrational coupling and to separate different line-broadening mechanisms in molecular systems [10–19]. More recently, this technique has been applied to study exciton correlations in semiconductor quantum wells [20–26]. It has been shown that a single two-dimensional spectrum can reveal couplings between resonances, separate quantum mechanical pathways, and distinguish the microscopic mechanisms of many-body interac-

\* Corresponding author. Tel.: +1 303 492 7858; fax: +1 303 735 0101.

E-mail address: [cundiff@jila.colorado.edu](mailto:cundiff@jila.colorado.edu) (S.T. Cundiff).

tions between excitons. Information about coupling and many-body contributions can be obtained by other enhancements to transient four-wave mixing, such as time-resolving the signal [27], spectrally resolving the signal [28] or measuring the full polarization resolved dynamics using dual channel spectral interferometry [29]. However, 2D-FT spectra provide clearer separation of different contributions and identification of the many-body contributions, particularly in complex situations, such as the one studied here.

Optical 2D-FT spectroscopy is still in an early stage of development. New understanding of the technique itself may be obtained by studying DQWs with engineered energy bands. For example, the conduction or valence subbands of DQWs can be brought into resonance by applying an electric field along the growth direction of the quantum well. It is then possible to initiate enhanced coherent oscillations of electron, hole or exciton wavepackets [30]. Such studies may show how wavepacket oscillations are manifested in 2D-FT spectra. This has implications for interpreting recent experiments aimed at understanding the ultrafast dynamics of other chemical systems, e.g., hydrogen bonds in solvents [31,32].

## 2. 2D Fourier transform spectroscopy

2D-FT spectroscopy is a heterodyne-detected four-wave-mixing (FWM) technique that records and correlates phase evolution during two controlled time periods, an initial evolution period,  $\tau$ , and a final signal detection period,  $t$ , separated by a certain mixing (or waiting) time,  $T$ , as illustrated in Fig. 1(a). A Fourier transform with respect to  $\tau$  and  $t$  yields a 2D spectrum as a function of absorption frequency  $\omega_\tau$  and emission frequency  $\omega_t$ , respectively. The FWM signal,  $S(\tau, T, t)$  is a function of three time variables. More generally, it could be transformed to a three-dimensional spectrum,  $S(\omega_\tau, \omega_T, \omega_t)$ . The 2D spectra we present here are slices of the general 3D spectrum corresponding to holding  $T$  constant, i.e., they are  $S(\omega_\tau, T, \omega_t)$ .

A peak in a 2D spectrum indicates that an oscillation at absorption frequency  $\omega_\tau$  during the initial time period gives rise to an oscillation at emission frequency  $\omega_t$  during the third period. Coupling between resonances can be identified by the presence of cross peaks in the 2D spectrum ( $\omega_\tau \neq \omega_t$ ). The intensity and shape of cross peaks reveal information regarding the coupling strength, dephasing dynamics, and Coulomb correlations between relevant resonances.

All discussion and measurements presented in this paper are based on the photon-echo pulse sequence, where the system evolves in conjugate frequencies during the time periods  $\tau$  and  $t$ . The phase of the FWM signal is given by  $e^{i(-\omega_\tau \tau + \omega_t t)}$ , where the absorption frequency has the opposite sign of the emission frequency. This allows cancelation of inhomogeneous dephasing within an ensemble of static distributed oscillation frequencies. Therefore, the spectra generated by this pulse sequence are often designated as “rephasing”.

A few schematic amplitude spectra representing different scenarios are presented in Fig. 1. They correspond to (b) two independent 2-level systems, (c) two 2-level systems coupled via incoherent relaxation processes, and (d) two excited states coupled via a common ground state. Typically, coherent coupling induced cross peaks appear instantly at  $T = 0$  whereas cross peaks due to incoherent relaxation processes are only observable at a finite waiting time ( $T > 0$ ).

The experimental set-up is described in detail elsewhere [20]. Three collinearly polarized pulses are configured in the phase-matched “box” geometry. The signal is detected in the background-free direction  $\mathbf{k}_s = -\mathbf{k}_a + \mathbf{k}_b + \mathbf{k}_c$ . The heterodyne-detected FWM signal field is completely characterized in amplitude and phase via

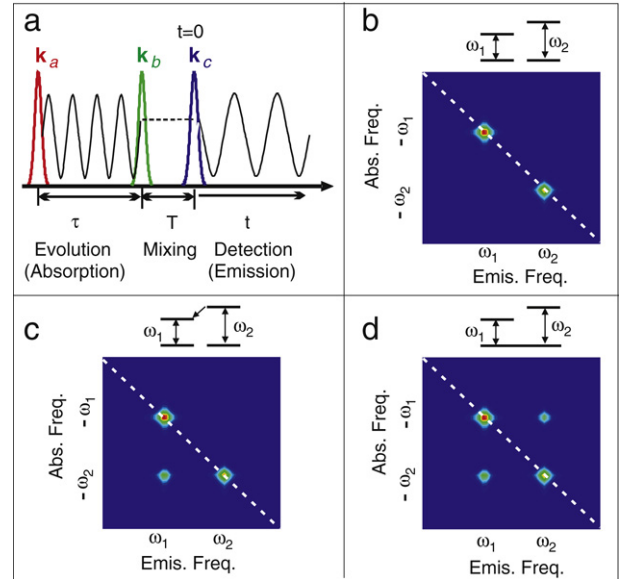


**Fig. 1.** (a) Pulse sequence and phase evolution of the polarization field in a typical 2D experiment. Schematic amplitude spectra for (b) two independent 2-level systems, (c) two 2-level systems coupled via incoherent relaxation processes, and (d) a 3-level system in a “V” configuration where two excited states are coupled via a common ground state. (b)–(d) are not results of rigorous simulations of a particular physical system, but schematics to represent possible ideal 2D spectra.

spectral interferometry. The FWM signal is combined collinearly with a phase-stabilized reference pulse and sent to a spectrometer. The spectral interferogram between the FWM and reference beam is measured by a CCD camera. The emission frequency,  $\omega_t$ , is obtained directly via the spectrometer. The indirect absorption frequency axis,  $\omega_\tau$ , is obtained by Fourier transform with respect to  $\tau$ . To obtain one 2D spectrum,  $T$  is fixed at a certain value, and  $\tau$  is varied with a step size of  $\sim 1$  fs for a few thousand steps. The experimental challenges mainly lie in maintaining phase stability ( $\sim \frac{\lambda}{80}$ ) between multiple pulse pairs and step delay  $\tau$  with sub-wavelength precision. We meet the requirements of having a phase stable reference and high precision stepping of  $\tau$  by implementing actively stabilized interferometers [20].

## 3. Electronic transitions in double quantum wells

We investigated two different DQW samples, both consisting of 10 periods of alternating 8 and 9 nm GaAs quantum wells. The barrier ( $\text{Al}_{0.3}\text{Ga}_{0.7}\text{As}$ ) thickness is 10 nm in sample A (thick barrier, weak coupling) and 1.7 nm in sample B (thin barrier, strong coupling), respectively. We calculate separately the single particle eigenstates of the conduction band, heavy-hole ( $hh$ ) and light-hole ( $lh$ ) valence bands, due to the one-dimensional quantum confinement in the growth direction. The single particle picture is approximate in that it neglects the Coulomb interaction between the electrons and holes. This interaction leads to the formation of excitons, or electron–hole pairs and higher order many-body effects. The binding energy of excitons depends on the materials and the thickness of quantum wells among other factors. For the quantum wells used in the current studies, the exciton binding energy is  $\sim 10$  meV. The purpose of this calculation is not to reproduce the energetic positions of experimentally observed resonances precisely, but to qualitatively discuss possible optically allowed transitions.

We have used a self-consistent solution of the one-dimensional solution Schrödinger equation [33–35]. In the calculation, we used the following effective masses  $m_e = 0.067$ ,  $m_{hh} = 0.48$ ,  $m_{lh} = 0.082$  and a band-gap of 1.5 eV for GaAs. We also used effe-

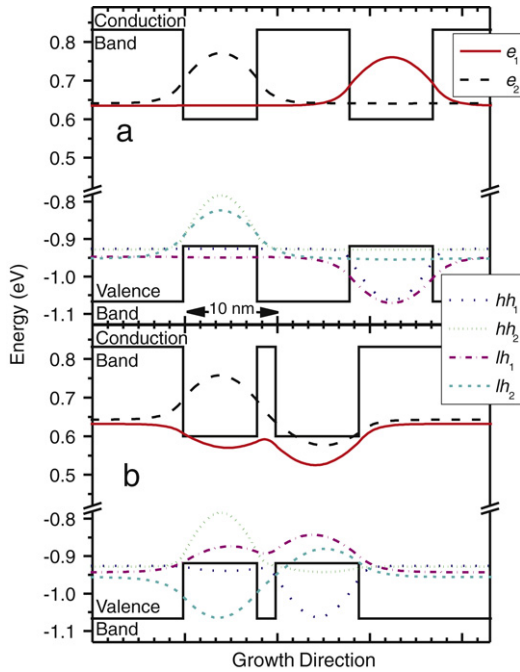


**Fig. 2.** Schematics of the DQW of 8 nm (left well) and 9 nm (right well) and calculated electron and hole wavefunctions for the case of 10 nm (a) and 1.7 nm (b) barriers. The wavefunctions are offset by the confinement energy of the state.

ctive masses  $m_e = 0.092$ ,  $m_{hh} = 0.489$ ,  $m_{lh} = 0.084$ , a band-gap of 1.798 eV for AlGaAs and a conduction band offset of 232 meV.

Electron and hole wavefunctions for the two DQW structures with thin and thick barriers are plotted in Fig. 2(a) and (b), respectively. In DQWs with thick barriers, electrons and holes are mainly localized in individual quantum wells. In DQWs with thin barriers of only 1.7 nm, the wavefunctions of the electrons and light-holes become extended into both wells, while the heavy-hole wavefunction remains mostly localized in individual wells. The lowest (second lowest) electron and hole energy states correspond to those wavefunctions localized in the wide (narrow) quantum well.

The strength of an optical transition is measured by the dipole moment between ground and excited states, which is proportional to the electron and hole wavefunction overlap. We have calculated the wavefunction overlap for many possible transitions between the valence and conduction bands in the DQW structure but listed only those with large values of overlap integrals. These “bright” transitions are plotted in Fig. 3 as functions of barrier thickness.

In the thick barrier DQW, four transitions have large dipole moments. In the order of increasing energy, these transitions are  $hh_1 \rightarrow e_1$ ,  $hh_2 \rightarrow e_2$ ,  $lh_1 \rightarrow e_1$ , and  $lh_2 \rightarrow e_2$ . To remind the reader that the experimentally observed resonances correspond to exciton transitions, we denote these peaks as  $EX_{hh1e1}$ ,  $EX_{hh2e2}$ ,  $EX_{lh1e1}$  and  $EX_{lh2e2}$ , respectively.

In the thin barrier DQW, dipole moments for transitions between  $hh_2 \rightarrow e_1$  and  $hh_1 \rightarrow e_2$  increase since the electron wavefunctions are extended in both wells and overlap with the heavy-hole wavefunctions. The value of the overlap integrals of these two transitions is approximately 1/3 of the other four transitions. The splitting between the two heavy-hole to conduction band transitions is small and therefore unresolved in our measurements. We tentatively assign four resonances from the lower to higher energies as  $hh_1/hh_2 \rightarrow e_1$ ,  $lh_1 \rightarrow e_1$ ,  $hh_1/hh_2 \rightarrow e_2$  and  $lh_2 \rightarrow e_2$ . Again, to emphasize that experimentally observed resonances are exciton transitions, we denote these transitions as  $EX_{hhe1}$ ,  $EX_{lh1e1}$ ,  $EX_{hhe2}$ ,  $EX_{lh2e2}$ , respectively. The accurate assignment of these resonances is difficult due to complications caused by

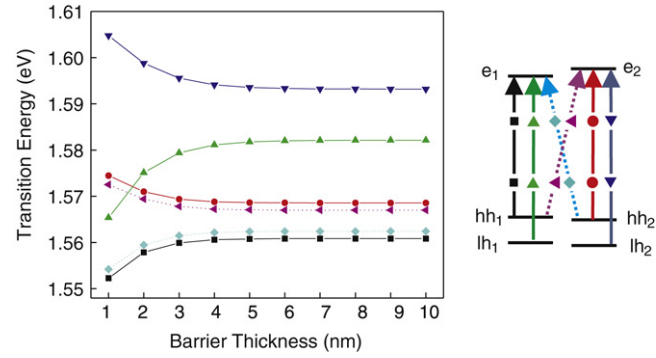


**Fig. 3.** Energy of optical transitions as a function of barrier thickness, calculated based on one-dimensional quantum confinement in the growth direction. Two transitions indicated by dotted line are only allowed when the barrier is thin and the wavefunctions become extended in both wells. Diagram at right shows the transitions between single particle states.

valence band mixing and energy shifts due to strain, which can vary from sample to sample.

#### 4. Experimental results

We first perform measurements using traditional spectrally resolved and time-integrated FWM techniques. All data are taken at a sample temperature of 10 K. Four distinct resonances in spectrally-resolved FWM measurements are observed in both sample A and sample B. In the notation introduced above, spectrally-resolved FWM corresponds to  $S(\tau = 0, T = 0, \omega_t)$ . The data for sample B are shown in Fig. 4(a). We then perform time-integrated FWM measurements on sample B, where the time-integrated signal is  $S_{TI}(\tau) = \int S(\tau, T = 0, t) dt$ . A weak oscillatory signal was observed, as shown in Fig. 4(b). These oscillations may arise from macroscopic polarization interferences or quantum beats due to genuine quantum mechanical coupling [27,36,37]. Quantum beats are typically identified as spectroscopic signatures for the presence of electronic coupling. There are, however, several inherent limitations in using the beating behavior to extract information on electronic coupling. First, it is often difficult to distinguish macroscopic classical polarization interference from microscopic quantum beats. Secondly, one usually analyzes the oscillation periods to identify the energy splitting between the coupled resonances. The oscillations, however, can disappear very quickly, due to both the loss of quantum coherence and destructive interference, so that a reliable analysis of the oscillation periods is often difficult. Finally, if multiple resonances with similar splitting are present, it is almost impossible to identify which particular resonances are coupled. These limitations are demonstrated clearly in the conventional time-integrated FWM measurements, as shown in Fig. 4(b). In contrast, 2D-FT spectroscopy allows one to circumvent these limitations. As a result, we were able to establish the presence of electronic couplings and to determine the coherent or incoherent nature of these couplings between specific transitions without any ambiguity.

In DQWs with thick barriers, there are several possible coupling mechanisms between various electronic resonances. In this case, electron and hole wavefunctions are localized in individual quantum wells. No coupling is expected between exciton resonances in different quantum wells. Heavy-hole and light-hole transitions confined in the same quantum well are expected to be coupled, since the same conduction band energy level is involved. Thus one expects a spectrum similar to that shown in Fig. 1(d). Such heavy-hole and light-hole couplings in single quantum wells have been extensively studied and investigated via both conventional FWM techniques and 2D-FT

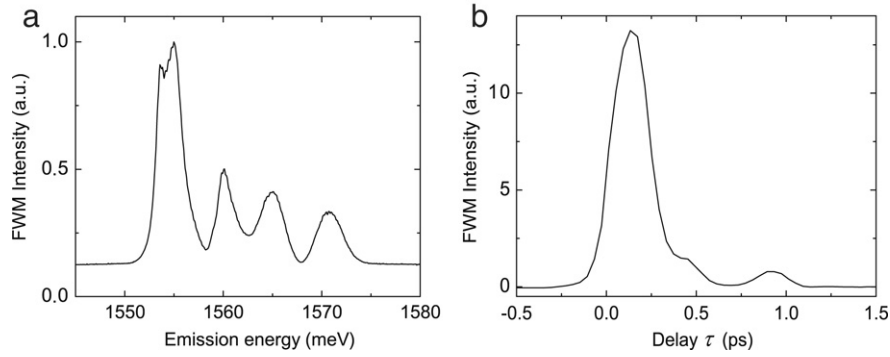


**Fig. 4.** (a) Spectrally-resolved FWM signal ( $S(\tau = 0, T = 0, \omega_t)$ ) and (b) time-integrated FWM signal ( $\int S(\tau, T = 0, t) dt$ ) taken on the sample B with 1.7 nm thin barriers.

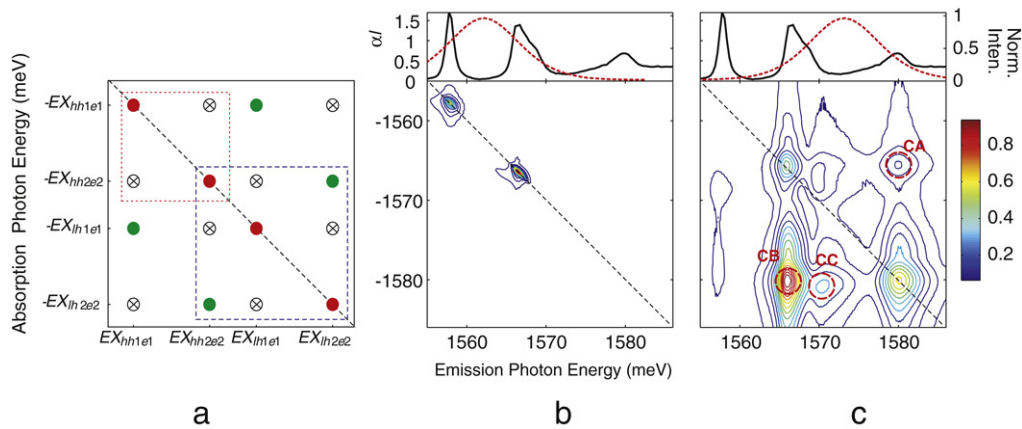


**Fig. 5.** (a) Expected 2D-FT amplitude spectrum for the sample A with 10 nm thick barriers; (b) Measured 2D-FT amplitude spectrum,  $|S(\omega_r, T, \omega_t)|$ , with laser tuned to the two resonances,  $EX_{hh1e1}$  and  $EX_{hh2e2}$ , at lower energy, corresponding to the area in the red box in (a); (c) Measured amplitude spectrum,  $|S(\omega_r, T, \omega_t)|$  with laser tuned to the three resonances,  $EX_{hh2e2}$ ,  $EX_{lh1e1}$ , and  $EX_{lh2e2}$ , at higher energy, corresponding to the area in the blue box in (a). Both measured spectra are taken at  $T = 6.67$  ps. Upper panels in (b) and (c) show the linear absorption spectrum (left axis) and laser spectrum (right axis). (For interpretation of the references to colour in this figure legend, the reader is referred to the web version of this article.)

spectroscopy [21,22]. In a simple picture, where only heavy-hole and light-hole coupling of the same quantum well is considered, we expect the 2D spectrum to resemble the one shown in Fig. 5(a). The red circles represent diagonal peaks, the green circles represent cross peaks between *hh* and *lh* excitons due to common electronic states, and the crosses indicate that no cross peaks are expected according to the simple analysis above.

The spectral bandwidth from our 150 fs Ti:Sapphire laser is less than 10 meV. Therefore, we cannot excite all four transitions in sample A simultaneously. In Fig. 5(b), the laser was tuned to overlap with the lowest two transitions,  $EX_{hh1e1}$  and  $EX_{hh2e2}$ . No cross peaks were observed, confirming that these two resonances are due to heavy-hole transitions localized in the two spatially-separated quantum wells ( $EX_{hh1e1}$  and  $EX_{hh2e2}$ ).

We then tuned the laser to cover the three transitions at higher energies and obtained the spectrum shown in Fig. 5(c). As expected, two cross peaks (CA and CB) were identified as coupling between  $EX_{hh2e2}$  and  $EX_{lh2e2}$  because they share a common conduction band state. The cross peak CA represents quantum pathways in which a lower energy transition is excited at the first and/or second perturbation order and the emission of a higher energy transition at the third order is subsequently influenced due to the phase space-filling or other coherent mechanisms. Another feature worth noting is that one cross peak (CB) has the strongest intensity. Similar features were observed in 2D spectra obtained on single quantum wells [21]. The intensity of a cross peak is expected to be in between those of the diagonal peaks in calculations based on simple level schemes. It is necessary to include higher order Coulomb correlations to account for the abnormally strong cross

peak. We also note a small spectral shift between a heavy-hole transition that is common in both Fig. 5(b) and (c). This shift is due to the fact that these two spectra are taken at different spatial locations on the sample. Spatially inhomogeneous strain causes the exact resonant energies to vary across the sample.

The appearance of the cross peak CC, which indicates coupling between the two LH exciton states, is surprising considering the large barrier thickness. This cross peak, which is present even when the waiting time,  $T$ , was set to be 200 fs (data not shown), likely arises from energy transfer. Whether or not energy transfer can happen effectively between excitons completely localized in spatially well separated quantum wells is not clear. A few possible transfer mechanisms include dipole-dipole interaction, intrinsic structural inhomogeneity, Auger process, and two-photon-absorption process. Dipole-dipole coupling typically has a short range and diminishes quickly after a few nanometers. The range of dipole-dipole interaction may be extended between excitons in spatially-separated DQWs either via phonon-assistance or via interface roughness [38]. The first mechanism is incoherent and destroys quantum coherence while the second mechanism is likely to partially preserve phase coherence between different excitation levels. Structural inhomogeneity in the barriers may also lead to coupling between excitons in spatially-separated DQWs. Low potential channels in the alloy barrier created by microscopic clustering of like molecules may exist, which enables percolation-like transport processes [39]. It has also been suggested that transfer may occur over the barriers due to Auger processes [40]. We cannot identify the exact coupling mechanism based on the measurements presented here. The fact that we observed only

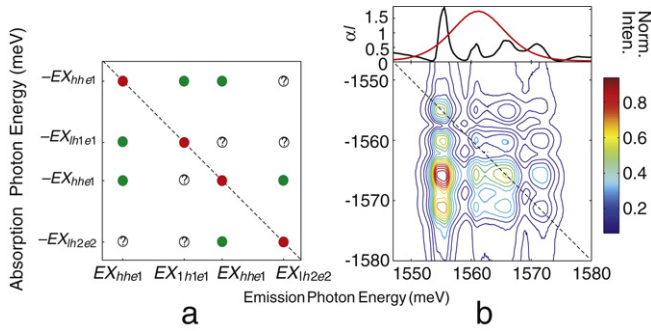


**Fig. 6.** (a) An expected 2D-FT amplitude spectrum for sample B; (b) A measured 2D-FT amplitude spectrum,  $|S(\omega_r, T, \omega_t)|$  for  $T = 6.7$  ps. Upper panel is linear absorption spectrum (left axis) and laser spectrum (right axis).

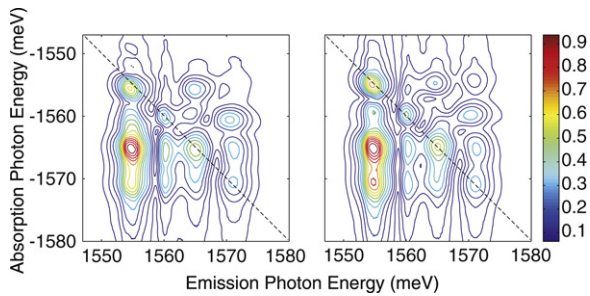


**Fig. 7.** Amplitude spectra,  $|S(\omega_r, T, \omega_t)|$  of sample B with 1.7 nm thin barriers measured at different waiting times. (a)  $T = 280$  fs; (b)  $T = 400$  fs are chosen at a maximal and a minimal point of oscillations observed in the time-integrated FWM measured as a function  $T$ .

one cross peak below the diagonal suggests that the coupling mechanism between two light-hole resonances may be incoherent relaxation. If this is the case, the energy transfer or relaxation happens very fast, on a time scale shorter than our pulse. However, we have previously observed asymmetry between the cross peaks that arises due to a combination of different dephasing times and many-body effects [24].

In DQWs with thin barriers of only 1.7 nm, we again observed four resonances in spectrally-resolved FWM measurements as shown in Fig. 4(a). It is difficult to resolve all transitions because of the small energy splitting between two heavy-hole levels. We assigned the four peaks as  $EX_{hhe1}$ ,  $EX_{lh1e1}$ ,  $EX_{hhe2}$ ,  $EX_{lh2e2}$ , respectively, from lower to higher energies. We provide an expected 2D spectrum shown in Fig. 6(a) considering only “common state” coupling as the possible origin of cross peaks. Due to the difficulties in assigning the transitions, it is not clear if some of the transitions are coupled. The measured amplitude spectrum, taken at  $T = 6.7$  ps is shown in Fig. 6(b). A grid pattern is observed, suggesting that all resonances are coupled with one another. The measured spectrum indicates that there are valence band mixing effects, which are not taken into consideration in our simple single particle calculations. Such valence band mixing would couple  $hh$  and  $lh$  states and explain the observed spectrum.

Interesting changes in cross-peak intensities are observed as functions of the waiting time, as shown in Fig. 7. These changes can be explained by the interference between different quantum mechanical pathways that contribute to the cross peaks. In particular, there are two types of terms that contribute to the cross peaks in our experimental geometry. They are referred to as the “ground state bleaching” and “excited state emission” terms, respectively [25]. The “excited state emission” terms, when appearing at the cross-peak positions, include a stimulated Raman coherence (a non-radiative coherence between the heavy-hole and light-hole states). This Raman coherence gives rise to a slowly varying phase, proportional to  $e^{i\delta\omega T}$ , during the mixing (or the

waiting) period [41]. As the waiting time  $T$  is varied, the phase of the Raman coherence terms changes, leading to destructive or constructive interference with the quantum mechanical pathways due to the “ground state bleaching” terms. In the case that the cross-peak intensity is strongly modified by higher order Coulomb correlation, such Raman coherence oscillatory behavior may be masked and difficult to observe. We note that such oscillatory behavior in cross-peak intensities has been reported recently in 2D-FT spectra on electronic transitions in photosynthetic systems [42]. In addition, it has recently been demonstrated that Raman coherences can be isolated in 2D spectra by measuring  $S(\tau, \omega_t, \omega_t)$  [43].

## 5. Summary

In summary, we have observed a rich variety of electronic coupling phenomena in our 2D-FT spectroscopy measurements performed on DQW samples with different barrier thicknesses. Coupling between heavy-hole and light-hole resonances confined in the same quantum well was identified in all samples. Heavy-hole resonances localized in spatially-separated quantum wells are not coupled in the sample with thick barriers of 10 nm. A somewhat surprising coupling between the light-hole resonances is observed, although excitons are confined in individual quantum wells separated by thick barriers. The origin of this coupling may be incoherent relaxation happening on a very fast time scale, short than our pulse duration,  $\sim 150$  fs. All heavy-hole and light-hole resonances become strongly coupled in the sample with thin barriers of 1.7 nm because electron wavefunctions are extended in both wells and the resonances now share common electron or hole states. In addition, cross-peak intensity oscillations as functions of the waiting time,  $T$ , occur. These oscillations, observable only under certain circumstances, can be explained by the slowly oscillating Raman coherence term as  $T$  is varied.

It is difficult to provide a detailed comparison between theoretical and experimental studies on the DQW structures used in current experiments. The small energy splitting between different valence band states makes the assignment of the observed resonances difficult. In the future, we would like to study DQW structures based on different materials so that heavy-hole and light-hole resonances are well separated. We also plan to apply an electric field to controllably introduce wavepacket oscillations and observe their manifestations in 2D spectra.

## Acknowledgments

We would like to thank Martin Koch for helpful discussions. The work at JILA and UCI was supported by the Chemical Sciences, Geosciences, and Energy Biosciences Division, Office of Basic Energy Science, Office of Science, U.S. Department of Energy and the National Science Foundation. S.T.C. is a staff member in the NIST Quantum Physics Division. X. Li gratefully acknowledges funding from ARO, NSF, and the Welch Foundation.

## References

- [1] H.W. Liu, R. Ferreira, G. Bastard, C. Delalande, J.F. Palmier, B. Etienne, Optical evidences of assisted tunneling in a biased double quantum well structure, *Appl. Phys. Lett.* 54 (1989) 2082–2084.
- [2] D.J. Leopold, M.M. Leopold, Tunneling-induced optical nonlinearities in asymmetric  $Al_{0.3}Ga_{0.7}As/GaAs$  double-quantum-well structures, *Phys. Rev. B* 42 (1990) 11147–11158.
- [3] D.Y. Oberli, J. Shah, T.C. Damen, J.M. Kuo, J.E. Henry, J. Lary, S.M. Goodnick, Optical phonon-assisted tunneling in double quantum well structures, *Appl. Phys. Lett.* 56 (1990) 1239–1241.
- [4] T. Westgaard, Q.X. Zhao, B.O. Fimland, K. Johannessen, L. Johnsen, Optical properties of excitons in  $GaAs/Al_{0.3}Ga_{0.7}As$  symmetric double quantum wells, *Phys. Rev. B* 45 (1992) 1784–1792.
- [5] J. Khurgin, Electro-optical switching and bistability in coupled quantum wells, *Appl. Phys. Lett.* 54 (1989) 2589–2591.

- [6] A. Zrenner, E. Beham, S. Stüfler, F. Findeis, M. Bichler, G. Abstreiter, Coherent properties of a two-level system based on a quantum-dot photodiode, *Nature* 418 (2002) 612–614.
- [7] X. Li, Y. Wu, D. Steel, D. Gammon, T.H. Stievater, D.S. Katzer, D. Park, C. Piermarocchi, L.J. Sham, An all-optical quantum gate in a semiconductor quantum dot, *Science* 301 (2003) 809–811.
- [8] S.T. Cundiff, Coherent spectroscopy of semiconductors, *Opt. Express* 16 (2008) 4639–4664.
- [9] R. Ernst, G. Bodenhausen, A. Wokaun, Principles of Nuclear Magnetic Resonance in One and Two Dimensions, Oxford Science Publications, Oxford, 1987.
- [10] Y. Tanimura, S. Mukamel, Two-dimensional femtosecond vibrational spectroscopy of liquids, *J. Chem. Phys.* 99 (1993) 9496–9511.
- [11] P. Hamm, M. Lim, R. Hochstrasser, Structure of the amide I band of peptides measured by femtosecond nonlinear-infrared spectroscopy, *J. Phys. Chem. B* 102 (1998) 6123–6138.
- [12] M.C. Asplund, M.T. Zanni, R.M. Hochstrasser, Two-dimensional infrared spectroscopy of peptides by phase-controlled femtosecond vibrational photon echoes, *Proc. Natl. Acad. Sci. USA* 97 (2000) 8219–8224.
- [13] S. Mukamel, Multidimensional femtosecond correlation spectroscopies of electronic and vibrational excitations, *Annu. Rev. Phys. Chem.* 51 (2000) 691–729.
- [14] O. Golonzka, M. Khalil, N. Demirdöven, A. Tokmakoff, Vibrational anharmonicities revealed by coherent two-dimensional infrared spectroscopy, *Phys. Rev. Lett.* 86 (2001) 2154–2157.
- [15] T. Brixner, J. Stenger, H. Vaswani, M. Cho, R. Blankenship, G. Fleming, Two-dimensional spectroscopy of electronic couplings in photosynthesis, *Nature* 434 (2005) 625–628.
- [16] D. Jonas, Two-dimensional femtosecond spectroscopy, *Annu. Rev. Phys. Chem.* 54 (2003) 425–463.
- [17] R.M. Hochstrasser, Two-dimensional spectroscopy at infrared and optical frequencies, *Proc. Natl. Acad. Sci. USA* 104 (2007) 14190–14196.
- [18] M. Cho, Coherent two-dimensional optical spectroscopy, *Chem. Rev.* 108 (2008) 1331–1418.
- [19] P. Hamm, J. Helbing, J. Bredenbeck, Two-dimensional infrared spectroscopy of photoswitchable peptides, *Annu. Rev. Phys. Chem.* 59 (2008) 291–317.
- [20] T.H. Zhang, C.N. Borca, X.Q. Li, S.T. Cundiff, Optical two-dimensional Fourier transform spectroscopy with active interferometric stabilization, *Opt. Express* 13 (2005) 7432–7441.
- [21] C.N. Borca, T.H. Zhang, X.Q. Li, S.T. Cundiff, Optical two-dimensional Fourier transform spectroscopy of semiconductors, *Chem. Phys. Lett.* 416 (2005) 311–315.
- [22] X.Q. Li, T.H. Zhang, C.N. Borca, S.T. Cundiff, Many-body interactions in semiconductors probed by optical two-dimensional Fourier transform spectroscopy, *Phys. Rev. Lett.* 96 (2006) 057406.
- [23] T. Zhang, I. Kuznetsova, T. Meier, X. Li, R. Mirin, P. Thomas, S. Cundiff, Polarization-dependent optical 2d fourier transform spectroscopy of semiconductors, *Proc. Natl. Acad. Sci.* 104 (2007) 14227–14232.
- [24] I. Kuznetsova, P. Thomas, T. Meier, T. Zhang, X. Li, R.P. Mirin, S.T. Cundiff, Signatures of many-particle correlations in two-dimensional Fourier-transform spectra of semiconductor nanostructures, *Solid State Commun.* 142 (2007) 154–158.
- [25] L.J. Yang, I.V. Schweigert, S.T. Cundiff, S. Mukamel, Two-dimensional optical spectroscopy of excitons in semiconductor quantum wells: Liouville-space pathway analysis, *Phys. Rev. B* 75 (2007) 125302.
- [26] M. Eremenchouk, M.N. Leuenberger, L.J. Sham, Many-body interaction in semiconductors probed with two-dimensional Fourier spectroscopy, *Phys. Rev. B* 76 (2007) 115307.
- [27] M. Koch, J. Feldmann, G. von Plessen, E.O. Göbel, P. Thomas, K. Köhler, Quantum beats versus polarization interference – an experimental distinction, *Phys. Rev. Lett.* 69 (1992) 3631–3634.
- [28] V.G. Lyssenko, J. Erland, I. Balslev, K.H. Pantke, B.S. Razbirin, J.M. Hvam, Nature of nonlinear 4-wavemixing beats in semiconductors, *Phys. Rev. B* 48 (1993) 5720–5723.
- [29] A.L. Smirl, M.J. Stevens, X. Chen, O. Buccafusca, Heavy-hole and light-hole oscillations in the coherent emission from quantum wells: Evidence for exciton–exciton correlations, *Phys. Rev. B* 60 (1999) 8267–8275.
- [30] K. Leo, J. Shah, E.O. Göbel, T.C. Damen, S. Schmitt-Rink, W. Schäfer, K. Köhler, Coherent oscillations of a wave packet in a semiconductor double-quantum-well structure, *Phys. Rev. Lett.* 66 (1991) 201–204.
- [31] C. Fecko, J. Eaves, J. Loparo, A. Tokmakoff, P. Geissler, Ultrafast hydrogen-bond dynamics in the infrared spectroscopy of water, *Science* 301 (2003) 1698–1702.
- [32] T. Steinel, J. Asbury, S. Corcelli, C. Lawrence, J. Skinner, M. Fayer, Water dynamics: dependence on local structure probed with vibrational echo correlation spectroscopy, *Chem. Phys. Lett.* 386 (2004) 295–300.
- [33] G.L. Snider, I.-H. Tan, E.L. Hu, Electron states in mesa-etched one-dimensional quantum well wires, *J. Appl. Phys.* 68 (1990) 2849–2853.
- [34] I.-H. Tan, G.L. Snider, L.D. Chang, E.L. Hu, A self-consistent solution of Schrödinger–Poisson equations using a nonuniform mesh, *J. Appl. Phys.* 68 (1990) 4071–4076.
- [35] Freeware for performing the calculations can be found on the website <http://www.nd.edu/gsnider/>.
- [36] X. Zhu, M.S. Hybertsen, P.B. Littlewood, Quantum beats in photon echo from four-waving mixing, *Phys. Rev. Lett.* 73 (1994) 209.
- [37] M. Koch, J. Feldmann, G. von Plessen, S.T. Cundiff, E.O. Göbel, P. Thomas, K. Köhler, Koch, et al., reply, *Phys. Rev. Lett.* 73 (1994) 210.
- [38] M. Batsch, T. Meier, P. Thomas, M. Lindberg, S.W. Koch, J. Shah, Dipole–dipole coupling of excitons in double quantum wells, *Phys. Rev. B* 48 (1993) 11817–11826.
- [39] D.S. Kim, H.S. Ko, Y.M. Kim, S.J. Rhee, S.C. Hohng, Y.H. Yee, W.S. Kim, J.C. Woo, H.J. Choi, J. Ihm, D.H. Woo, K.N. Kang, Percolation of carriers through low potential channels in thick  $\text{Al}_x\text{Ga}_{1-x}\text{As}_{0.35}$  barriers, *Phys. Rev. B* 54 (1996) 14580–14588.
- [40] R. Hellmann, A. Euteneuer, S. Hense, J. Feldmann, P. Thomas, E. Göbel, D. Yakovlev, A. Waag, G. Landwehr, Low-temperature anti-Stokes luminescence mediated by disorder in semiconductor quantum-well structures, *Phys. Rev. B* 51 (1995) 18053–18056.
- [41] A.G.V. Pivey, C.N. Borca, S.T. Cundiff, Correlation coefficient for dephasing of light-hole excitons and heavy-hole excitons in GaAs quantum wells, *Solid State Commun.* 145 (2008) 303–307.
- [42] G.S. Engel, T.R. Calhoun, E.L. Read, T.-K. Ahn, T. Mancal, Y.-C. Cheng, R.E. Blankenship, G.R. Fleming, Evidence for wavelike energy transfer through quantum coherence in photosynthetic systems, *Nature* 446 (2007) 782–786.
- [43] L. Yang, T. Zhang, A.D. Bristow, S.T. Cundiff, S. Mukamel, Isolating excitonic raman coherence in semiconductors using two-dimensional correlation spectroscopy, *J. Chem. Phys.* 129 (2008) 234711.